



## Experimental and CFD Analysis of Two-Phase Forced Convection Flow in Channels of Various Rib Shapes

Azher M. Abed<sup>1,\*</sup>, Doaa Fadhil Kareem<sup>1,2</sup>, Hasan Sh Majdi<sup>3</sup>, Ammar Abdulkadhim<sup>1</sup>

<sup>1</sup> Air conditioning and Refrigeration Techniques Engineering Department, Al-Mustaqbal University College, Babylon, 51001, Iraq

<sup>2</sup> Diwan Affairs Division, University of Baghdad, 10071, Baghdad, Iraq

<sup>3</sup> Department of Chemical Engineering and Petroleum Industries, Al-Mustaqbal University College, Babylon, 51001, Iraq

### ARTICLE INFO

#### Article history:

Received 8 January 2020

Received in revised form 18 August 2020

Accepted 23 August 2020

Available online 30 October 2020

### ABSTRACT

This paper investigates numerically and experimentally heat transfer forced convective two-phase flow (i.e. air and water) over a rectangular ribbed channel with a vertical orientation. Three distinct rib-groove shapes have been examined. Ribs - groove shapes are; Triangle, Trapezoid, and Semi-Trapezoid ribs-groove. The present study has been performed with continuous heat flux through range of water and air superficial inlet velocity values between 0.105 – 0.316m/s, and 0.263 – 1.320 m/s, respectively. Continuity, momentum and energy calculations have been formulated using the Finite Volume Approach (FVM). Results indicate that the triangle rib-groove has the high heat transfer coefficient and lower temperature difference than other cases against a different number of Reynolds. The experimental data has been compared to numerical results for ribs –grooved channel with deviation of about 1.0% - 7.5%. The channel fitted with triangle ribs shows the highest heat transfer, which is about 59% higher than the smooth channel; 56% for trapezoidal rib, and 44% for channel fitted by semi-trapezoidal rib. Finally, the triangle rib-groove gives a better heat transfer improvement value in comparison with trapezoidal and semi trapezoidal rib-groove channel at constant pumping power.

#### Keywords:

CFD; Rib-grooves; Rectangular channel;

Two-phase flow; turbulent flow

## 1. Introduction

Improvement of the efficiency of heat transfer of the heat exchangers with the use of the passive and active methods have been studied intensively numerically and experimentally during the last years due to their enhanced geometrical parameter such as ribs flowed through the grooves significantly enhanced the thermal performance and heat transfer rate [1-6]. An existing passive approach is defined by employing special surface geometries or fluid additives, and roughed surfaces anything that results in enhanced thermal performance. Whereas the active approaches comprise electric or acoustic fields, surface vibration, and mechanical aids merely the approaches requiring the

\* Corresponding author.

E-mail address: [azhermuhson@mustaqbal-college.edu.iq](mailto:azhermuhson@mustaqbal-college.edu.iq), [azhermuhson@gmail.com](mailto:azhermuhson@gmail.com)

external source of power [7]. A sufficient technique is using grooves or ribs in channels. Ribs design is dependent on the application. Ribbed channels are usually used to improve convection heat transfer in a range of applications such as refrigeration, nuclear energy, mechanical engineering, and heating systems. Due to the fact that the existence of the ribs in channels produced a flow of turbulence through breaking laminar sublayer in the case of comparing it against smooth channel, which results in increasing heat transfer rate. In addition to that, the thickness of the thermal boundary layer is decreased by ribs as a result of the areas of the secondary flow, appearing by the wall, as a result, increasing the rate of the heat transfer. This work may be carried out through the maintenance of roughness parts' height in comparison to the channel's dimensions [8, 9]. The behavior of flow and heat transfer coefficient in the ribbed and the smooth channels had been studied extensively by researchers such as [10-12]. However, the ribbed channels in various applications of engineering are more complicated than that of the smooth channels. Forced convection is the most commonly used method of heat transfer in a wide range of engineering applications and chemical processes. Wires, grooves, or ribs are fixed on the surface to get roughness elements for enhancing the heat transfer rate [9, 13]. The turbulent forced convective flow inside a 2-D channel by wall, have been reported by Eiamsa-ard and Promvonge [14]. Nine transverse grooves were located on the bottom channel wall.

The impact of geometrical shapes of grooves on rate of heat transfer of turbulent flow was studied by Ramadhan *et al.*, [15]. Four different shapes of grooves triangular, circular trapezoidal, and rectangular, were used. Fathinia *et al.*, [16], study theoretically, the impacts of various nano-particle kinds like Aluminum oxide ( $\text{Al}_2\text{O}_3$ ), Zinc oxide ( $\text{ZnO}$ ), and Silicon dioxide ( $\text{SiO}_2$ ) were reported with the water as the base fluid, on two-dimensions channel fitted with the grooves. Sivakumar *et al.* [17], determined the experimental Nusselt number and factor of friction data of airflow in a different rectangular channel with an angle of inclination equal to  $1^\circ$  in the  $y$ -direction had a smooth rib, and then fitted with different height ribs of (3, 6, and 9 mm). Fifi *et al.*, and Salman [18, 19], conducted a numerical analysis for studying the impacts of various shapes of ribs like (triangular, trapezoidal, and rectangular), on forced heat transfer of the convection and friction factor in the rectangular duct. Kim *et al.*, [20], performed numerical study for determining the impacts of entrance velocity of coolant flow on the flow and convection heat transfer features in ribbed ducts. Eiamsa and Promvonge [21], studied the impacts of ribs-grooved compound tabulator on the forced heat transfer coefficient within a rectangular ribbed duct under regular heat flux conditions. Abdulrazzaq *et al.*, [22], employed a CFD model to research the effects of triangle ribs of various angles ( $45^\circ$ ,  $60^\circ$ , and  $90^\circ$ ) on heat transfer rates of turbulent water flow. Habeeb and Al-Turaihi [23], investigated the two phases (air-water) flow around triangular – section obstacle in rectangular channel experimentally and numerically for steady and unsteady flows. The influences of different ribs heights and angles of inclination on local heat transfer coefficients in vertical channel had been studied experimentally by Salameh [24], and then compared to those of the smooth channel without ribs.

In the present analysis, the experimental data were compared to the results obtained by the CFD simulation and a reasonable agreement was reached. The main aim of this investigation is studying experimentally and numerically the influence of using several values of the superficial velocity of (air and water) in addition to adding ribs inside channel on the distribution of the temperature and the coefficient of the forced local heat transfer. Also, compare the experimental and numerical results of the ribbed channel, Triangle, Trapezoidal, and Semi-Trapezoidal ribs-groove) with a smooth channel for a turbulent flow inside a vertical rectangular channel which is under to a constant heat flux.

## 2. The Experimental Set-up

Experiments have been carried out for examining the effects of the use of three shape of ribs-grooves on the features of the heat transfers of vertical rectangle channels. An experimental apparatus diagram has been illustrated in Figure 1. The rig test was made from the Pyrex material with a rectangular cross-section of  $(8.0 \times 3.0 \times 70.0\text{cm})$  with a  $(3.175\text{cm})$  diameter water pipe, and a  $(1.27\text{cm})$  diameter air pipe which was used for showing the mix behavior (i.e. the mix of water-air) around heated plate (rib-groove). The Ribs-groove are made from aluminum with thermal conductivity  $202.40 \text{ W/m k}$ . Three distinct Rib-groove shapes were used (Trapezoid, Triangle rib-triangle grooves, Semi-Trapezoidal Rib) as shown in Figure 2. Both the base width and bitch distance of the ribs-groove channel is held constant ( $b=1.4 \text{ cm}$ ) and the ribs-groove shapes were altered. The below height and width ranges will be investigated

- i. Channel height ( $h=70 \text{ cm}$ )
- ii. Rib height ( $h_r=0.8 \text{ cm}$ )
- iii. Channel width ( $W=3.0 \text{ cm}$ )
- iv. Rib width ( $W_r=11.0 \text{ cm}$ )
- v. Groove depth ( $d=0.5 \text{ cm}$ )
- vi. Groove width ( $W_g=11.0 \text{ cm}$ )

The rest of the equipment that have been utilized for experimental rig are listed below

- i. Main water tank of  $(1\text{m}^3)$  capacity.
- ii. Water pump with maximal  $(30\text{L}/\text{min})$  discharge and a maximum  $(30\text{m})$  head.
- iii. System of valves and piping  $(1.25\text{in})$ .
- iv. A water flow meter which is utilized for measuring the average of the water inflow that entered channel with a  $(0\text{L}/\text{min} - 35\text{L}/\text{min})$  range.
- v. The air compressor of type (Recomendamos Aceite/Worthington) with a  $(0.50\text{m}^3)$  specification capacity and  $(16 \text{ bar})$  maximum pressure which is utilized for providing the gas phase (i.e. the air) to test section. Meter of the air flow that has ranges from  $(0-25 \text{ L}/\text{min})$  was utilized to measure and control the amount of air flow rate.
- vi. AC power supply has been the power source for the heater of a plate-type, which is utilized to heat the external heated plate surface of test section. The Analyzers of the Digital Power have been utilized for balancing the electric voltage over heaters with a  $(260\text{V})$  max voltage.
- vii. The heater has been utilized for reaching a  $300\text{K}$  temperature on areas from each side with a  $(400\text{W at } 220\text{V})$  total power; K-type thermo-couples which have been fixed on channel over heated region has been utilized for measuring temperature.

Air and water as the test fluid, were directed into the systems at air discharge from  $2-8 \text{ l}/\text{min}$  and water discharge from  $5-12.5 \text{ l}/\text{min}$ . The operating speed of the compressor and the water pump was varied by using a series of valves and by-passages for the provision of wanted rates of air and water flow. Mixing is conducted at the inlet tube to facilitate a more consistent axial flow pattern before reaching the test section.

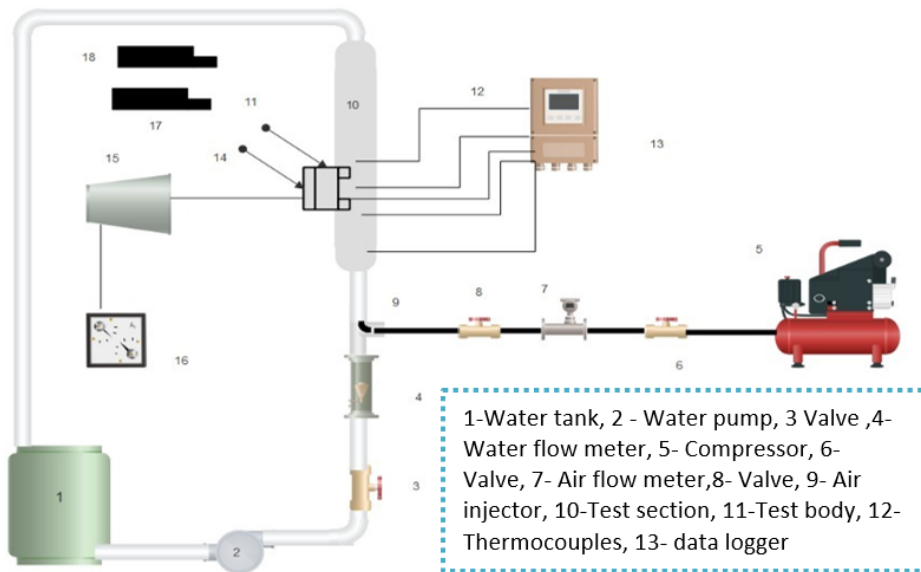


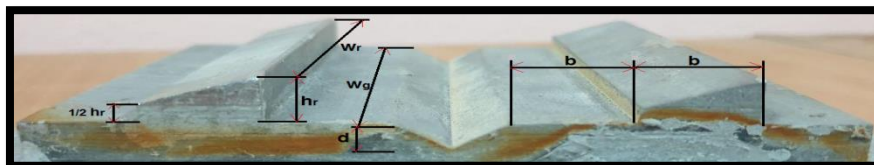
**Fig. 1.** Diagram of the test channel and measurement system



(a) Triangle Rib - Triangle Groove



(b) Trapezoidal Rib - Triangle Groove



(c) Triangle Groove-Semi-Trapezoidal Rib

**Fig. 2.** photographed of compound tabulator rib-grooved that used in the experimental work

### 3. The Processing of Data

The aim of the present experimentation is investigating the heat transfer coefficient in rectangular channel with the use of three different type of rib-groove tabulators. The independent parameters are flow rate and ribs-groove shapes. The coefficients of the local heat transfer are assessed from heat inputs and measured temperatures. With uniformly adding heat into the fluid ( $Q$ ) and the difference of the temperature between the wall and the fluid ( $T_s - T_b$ ), the coefficient of the local heat transfer is going to be assessed from experimental data through the use of the equations below [25, 26]

$$h = \frac{q}{\Delta T} \quad (1)$$

The temperature difference that used in this equation is  $(T_s - T_b)$ ,  $T_s$  is the heat plate temperature, measured with the use of the thermocouples. The bulk temperature ( $T_b$ ) at position  $Y$  along the direction of the flow and is measured on the assumption that the temperature of the linear working fluid rises along the rectangle channel and can be defined in the following form:

$$T_b = T_{in} + (T_{out} - T_{in}) \frac{Y}{L} \quad (2)$$

where  $T_s$ ,  $T_{in}$  and  $T_{out}$  were read from thermocouple output.

### 3.1 Numerical Methods

A “Computational fluid dynamic” CFD analysis of the 2-D simulation model of a two-dimensional rectangular geometry structure modeled with the energy equation and the Navier–Stokes equations. It is assumed that the fluid is turbulent, incompressible under steady state conditions without internal heat generation inside the channel. The governing equations for the continuity, energy, and momentum are required to be taken under consideration for full analysis of the CFD of rib–groove channel. The methodology used to solve these governing equations is described in the section below.

#### 3.2.1 Governing equations

Governing equations under previous conditions of (Navier-Stokes, Continuity, and Energy equations) are expressed as [27]

Continuity Equation

$$\frac{\partial}{\partial t}(\rho_m) + \nabla \cdot (\rho_m \vec{v}_m) = 0 \quad (3)$$

Momentum Equation

$$\frac{\partial}{\partial t}(\rho_m \vec{v}_m) + \nabla \cdot (\rho_m \vec{v}_m \vec{v}_m) = -\nabla P + \nabla \cdot [\mu_m (\nabla \vec{v}_m + \nabla \vec{v}_m^T)] + \rho_m \vec{g} + \vec{F} + \nabla \cdot \left( \sum_{k=1}^n \alpha_k \rho_k \vec{v}_{dr,k} \vec{v}_{dr,k} \right) \quad (4)$$

$n$  represents number of phases,  $\vec{F}$  represents a body force, and  $\mu_m$  represents the mix viscosity, expressed as

$$\mu_m = \sum_{k=1}^n \alpha_k \mu_k \quad (5)$$

### Energy Equation

$$\frac{\partial}{\partial t} \sum_{k=1}^n (\alpha_k \rho_k \mathbf{E}_k) + \nabla \cdot \sum_{k=1}^n (\alpha_k \vec{v}_k (\rho_k \mathbf{E}_k + \mathbf{P})) = \nabla \cdot (\mathbf{k}_{eff} \nabla T) + S_E \quad (6)$$

$k_{eff}$  represents effective conductivity ( $\sum \alpha_k (k_k + k_t)$ ), where  $k_t$  represents turbulent thermal conductivity. The first right-hand side term of Eq. (6) is the transfer of the energy as a result to the conduction.  $S_E$  includes any other volumetric sources of the heat.

#### 3.2.2 Standard $k$ - $\epsilon$ model

For the sake of attaining precise estimation in the channel of the ribs-groove, the standard mix model has been defined for the 2 model phases that may be characterized with the use of the following equations [27, 28]

$$\frac{\partial}{\partial t} (\rho_m k) + \nabla \cdot (\rho_m \vec{v}_m k) = \nabla \cdot \left( \frac{\mu_{t,m}}{\sigma_k} \nabla k \right) + G_{k,m} - \rho_m \epsilon \quad (7)$$

$$\frac{\partial}{\partial t} (\rho_m \epsilon) + \nabla \cdot (\rho_m \vec{v}_m \epsilon) = \nabla \cdot \left( \frac{\mu_{t,m}}{\sigma_\epsilon} \nabla \epsilon \right) + \frac{\epsilon}{k} (C_{1\epsilon} G_{k,m} - C_{2\epsilon} \rho_m \epsilon) \quad (8)$$

$\epsilon$  stands for the rate of the turbulent dissipation,  $\sigma$  stands for turbulent Prandtl number for  $k$  and  $\epsilon$ , and  $G^k$  represents the turbulence kinetic energy generation.

Turbulent viscosity,  $\mu_{t,m}$  and turbulence kinetic energy production,  $G_{k,m}$ , have been calculated using the following equations

$$\mu_{t,m} = \rho_m C_\mu \frac{k^2}{\epsilon} \quad (9)$$

$$G_{k,m} = \mu_{t,m} \left( \nabla \vec{v}_m + (\nabla \vec{v}_m)^T \right) : \nabla \vec{v}_m \quad (10)$$

The governing equations can be solved by utilizing CFD code FLUENT 15.0 with standard turbulence model of  $k$ - $\epsilon$  and SIMPLE algorithm. The criteria of convergence of  $10^{-6}$  and  $10^{-4}$  have been presumed respectively, for energy residuals and all other variables.

#### 3.3. Boundary Conditions

The boundary conditions for the present research have been defined for the rib-groove computational domain that have been illustrated in Figure 2. Those figures present the general model of the rib-groove channel which has been chosen from the present study, in which the left side wall at smooth and ribbed region is under a uniform heat flux ( $q''=100\text{W/m}^2$ ), whereas the remaining wall of the channel has been fixed as adiabatic. The upper edge of channel has been fixed to be an outlet pressure.

While the lower edge side is velocity inlet. The model of the turbulence is of a high importance for the accommodation of the behavior of the flow of every one of the applications. At inlet, the profile of the uniform velocity was imposed. The intensity of the turbulence has been set to 1% at inlet. The solutions have been thought of as converged in the case where normalized values of the residual reach  $10^{-5}$  for all of the variables.

### 3.4 Grid Independent Test

To check the numerical results' accuracy and validity, a grid-independent test has been carried out. Calculations have been performed with the use of 4 distinct sizes of the grid; 49470, 49384, 49260, and 21790 for channel fitted with triangular, trapezoidal, -trapezoidal, and smooth rib. Figure 3 illustrates the mesh of the smooth and channel with 3 rib types. The rectangular channel's geometry has been split into elements (i.e. to Quadrilateral structured grid) with the use of meshing which is combined with Ansys Work-bench 15 with a maximal and minimal size of 0.002m. The governing equations of the model would be solved at every one of the model geometry elements.

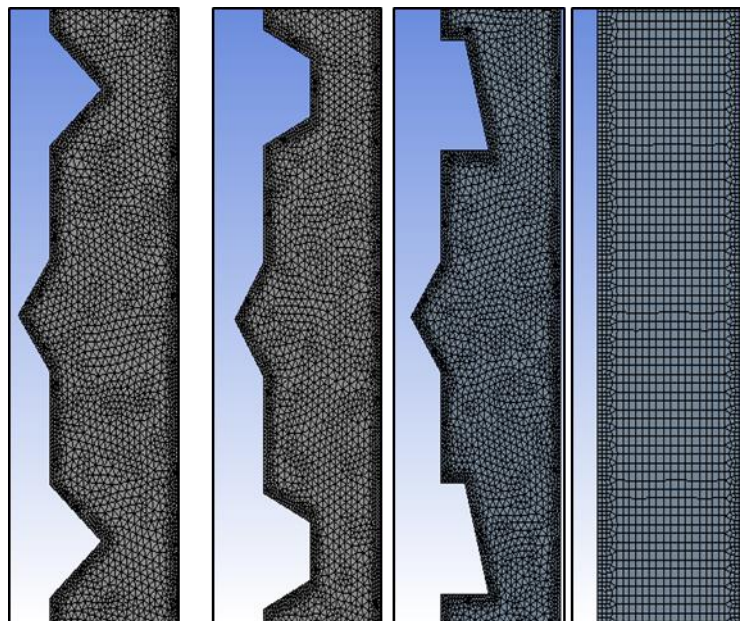
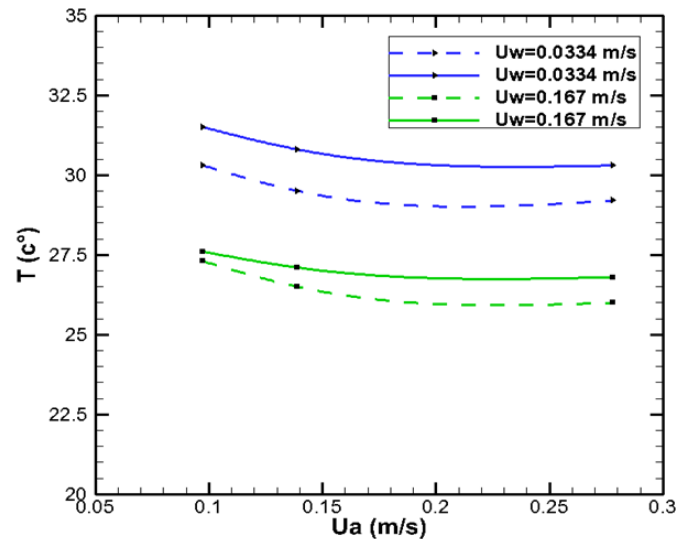


Fig. 3. Quadrilateral structured grid of computational domain

### 3.5 Validation of The Numerical Model

For the sake of proving the validity and accuracy for turbulence model and numerical procedure for this study, previous work for comparison between experimental and numerical values of exist temperature for Jalghaf, Al-Turaihi [28] has been performed as shown in Figure 4. Ansys Fluent 15.0 software was used to quantify numerically a two-dimensional heated body in a horizontal rectangular dimensional channel ( $8 \times 3 \times 70$  cm) to validate the model. The numerical temperature was compared with the experimental temperature from the work of other researchers. The validation trials were performed for 12 tests which consisted of (heated body, three air discharge 0.0972, 0.139, and 0.278 m/s, two water discharge 0.0334, and 0.167 m/s, and one heat flux 506 watt.



**Fig. 4.** Comparison between experimental and numerical values of exist temperature for Jalghaf, Al-Turaihi [28]

#### 4. Results and Discussions

In the present study, a forced convection of 2-phase flow (water and air) of heat transfer and temperature distribution over a rectangle ribbed channel with a vertical orientation was investigated. This research also investigated the impact of various ribs-groove shapes (triangular, trapezoidal, and semi-trapezoidal) at certain value of air superficial velocity on heat transfer behavior of the computational fluids. In addition to the heat transfer coefficient, the temperature distribution across the duct was carried out experimentally and numerically.

##### 4.1 Comparing Experimental and Numerical Heat Transfer Coefficient

Figure 5 to 7 present the comparison of experimental and numerical coefficient of local heat transfer for different shapes of rib-groove; triangular, trapezoidal, and semi-trapezoidal against various Reynolds numbers of water and air superficial. Moreover, it shows a comparison of experimental against numerical results for air and water superficial velocity 0.658m/s and 0.105m/s this pattern occurs at same coordinate in which the temperature sensors situated experimentally. The numerical results appeared to be having the same impact as experimental results with a (7.5 %) deviation that is found between them. The difference of the temperature reduces with the increase of the superficial velocity of the water based on the equation below

$$q = \dot{m} \cdot c_p \Delta T = VI - Q_{\text{loss}} \quad (11)$$

where

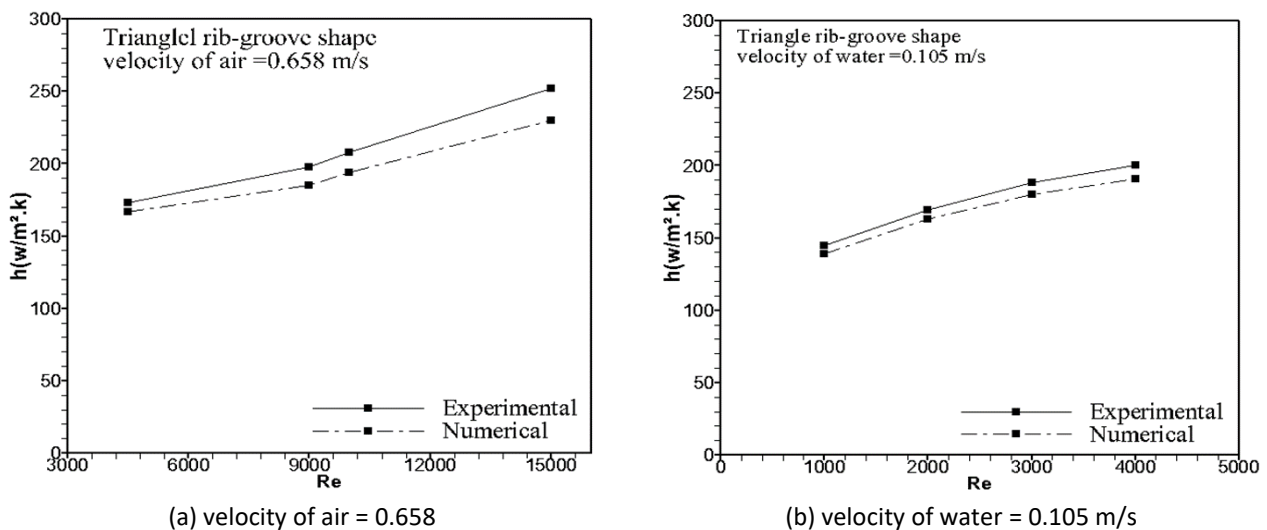
$$\dot{m} = \rho v A \quad (12)$$

The coefficient of heat transfer is found to be directly proportional to the velocity of the water superficially and inversely proportional to the difference in temperature, due to the fact that the



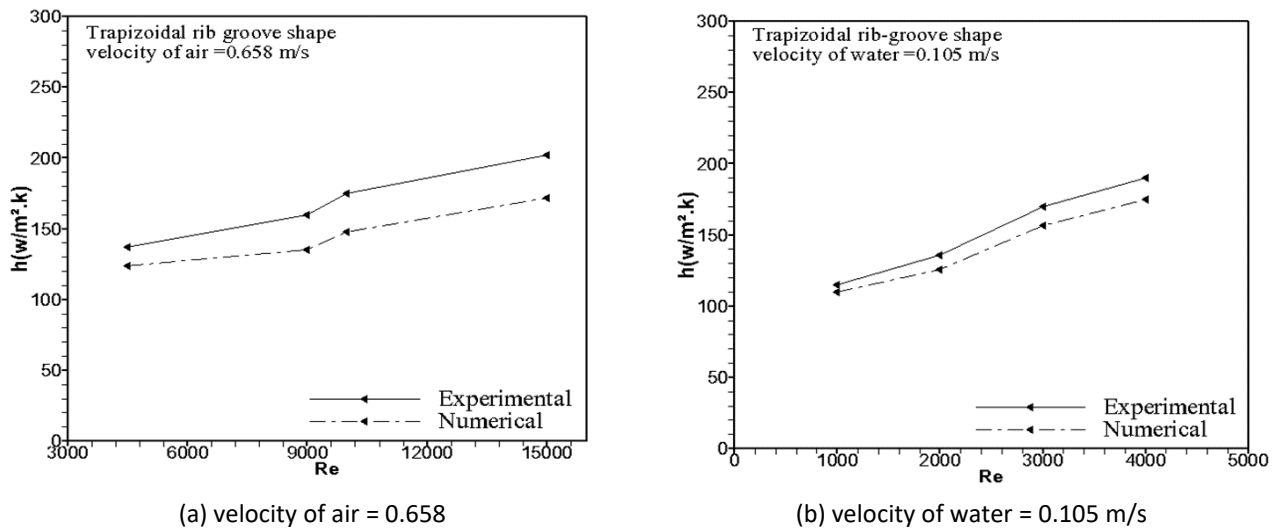
coefficient of heat transfer, as previously seen, increased the velocity of the water superficially and decreased the difference in temperature.

Figure 5(a) and 5(b), demonstrates a comparison of the local coefficient of heat transfer between the experimental and numerical results with different Re for Triangle rib-groove form at various air and water surface velocity values. It has been observed that the coefficient of the local heat transfer increased with the increase of the flow Reynolds number in presence the water and the mixture. The presence of air superficial increases the velocity of the mixing (warm and cold water) and as a result decreases the differences of the temperature between the wall and bulk water. The difference in temperature between the surface rib-groove and the cold mixture of water and air depending on the time of residence of the mixture within the tube. Due to the fact that the velocity of the water superficial raised from 0.105m/s to 0.316m/s, the value of experimental and numerical heat transfer coefficient increases from 171W/m<sup>2</sup>k to 252W/m<sup>2</sup>k, and from 167W/m<sup>2</sup>k to 230W/m<sup>2</sup> k, respectively. The reason for these phenomena can obtained due to the vortexes of the flow separation and reattachment to heat wall of rib-groove channel.



**Fig. 5.** Experimental and numerical heat transfer coefficient with different Re for Triangle rib-groove shape

Figure 6(a) and 6(b), shows the coefficient of the local heat transfer results for the channel which is fitted with the trapezoidal rib-groove shape, for several values of air and water superficial velocity at constant heat flux 0.658 m/s and 100 W, respectively. It has been noted that this difference increases with the increase in the water flow Reynolds number, and constant velocity of air of 0.658m/s which is from the minimum value 13 at the Re = 4500 up to the maximum value 30 at the Re = 15000. While, this difference slightly increases with the increase in the air flow Re number and 0.105m/s constant water velocity. This is due to that the fluid and turbulent mixing disturbance in the trapezoidal rib-groove channel is stronger when increasing the water flow rate than that of increasing the velocity of air through the channel, resulting in a stronger feature of the heat transfer at constant air velocity.



**Fig. 6.** Experimental and numerical heat transfer coefficient with different Re for Trapezoidal rib-groove shape

The effect of superficial air and water velocity on the characteristics of heat flow was illustrated in Figure 7(a) and 7(b). Experimental results were compared with numerical heat transfer coefficient of the channel which is fitted with semi-trapezoidal rib-groove shape, at constant heat flux. It has been found that the rate of heat transfer increases with the change of the surface velocity of water and air. It's seen in Figure 7(a) the heat transfer coefficient, in general, increases with change in the flow rate of the water for a given air superficial velocity for all rib groove shapes. This may result from an increase in the superficial velocity of the water and the mixture as a result of the air being pumped into the tube. This change in the velocity of the water and the mixture increases the friction level and the mixing motion of the water and the 2-phase air flow. The rate of heat transfer increases as the fluid velocity increases (good mixing in the turbulent boundary layer, thinner laminar sublayer). That's why 'Heat Transfer Coefficient' (which is a mixture of fluid, flow and body geometry) increased with an increase flow rate. At the other hand, the turbulent flow raises the air resistance and noise levels; however, the turbulent flow also accelerates heat conduction and thermal mixing [29]. Increasing the coefficient of the heat transfer with increasing the air Re number at constant superficial velocity of the water has been depicted in Figure 7(b) as well. It has been noted that the impacts of water superficial velocity on the rate of the heat transfer more than that of secondary flow by air superficial for all the type of rib groove channels. The presence of air bubbles increases the mixing (cold water and warm water) and thus reduces the temperature differences between the wall and the bulk water.

Increasing the air and water amounts in the channel leads to decrease the temperature difference and resulted in increasing local heat transfer coefficient according to Eq. (11) and (12), respectively. This reduction is attributed to the following: The air stream injection to water stream raises the level of the turbulence. The use of ribs-groove provides a high heat transfer surface area and prevents the creation of the boundary layer and produces a turbulent flow within the channel.

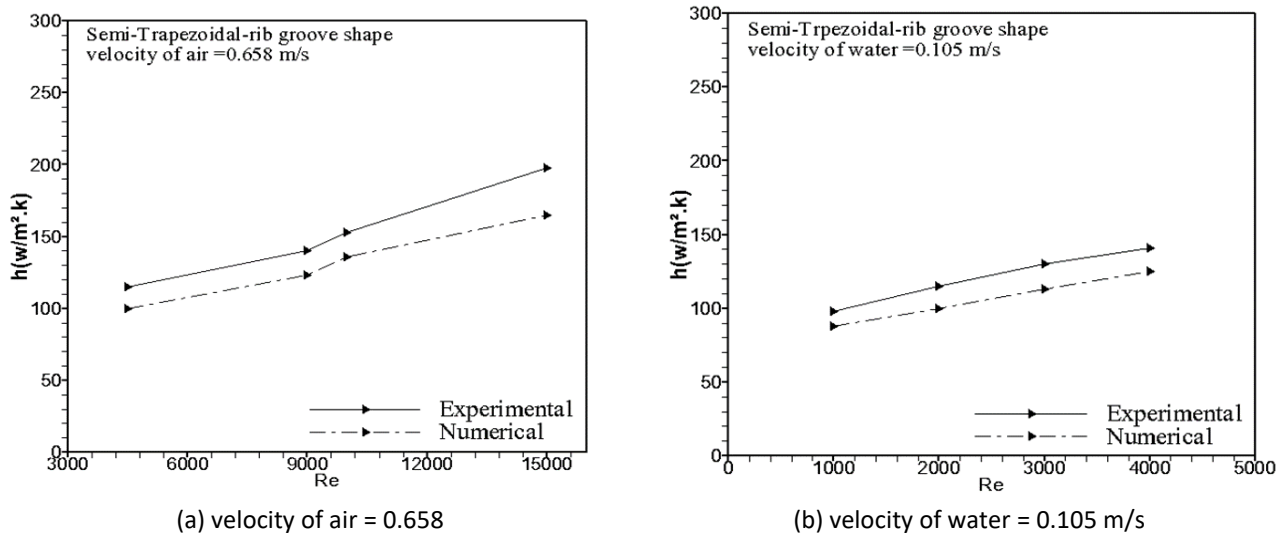


**Fig. 7.** Experimental and numerical heat transfer coefficient with different  $Re$  for Semi-Trapezoidal rib-groove shape

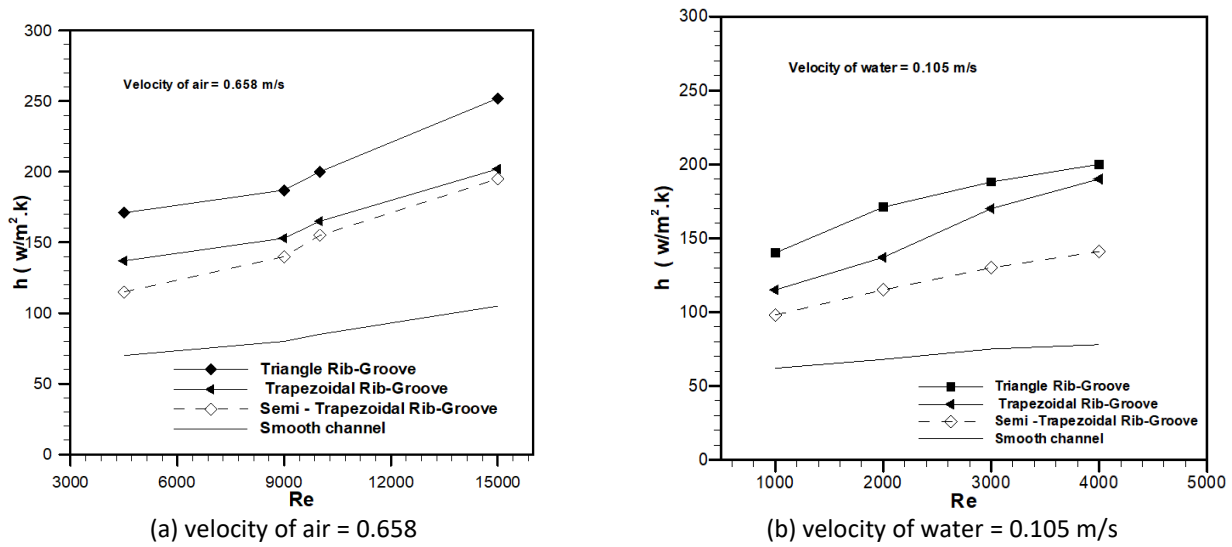
#### 4.2 Comparison Between Different Ribbed-Grooved Channels

For the sake of having an intuitive comprehension of the correlation between flow structure and convective transfer of heat in a rib-groove channels, Figure 8(a) and 8(b), illustrates comparing the coefficient of the heat transfer in 3 ribs channel types which have been resulted from the experimental results. It is observed that the every ribbed-groove shape has the maximum local heat transfer coefficient value in comparison to the smooth channel.

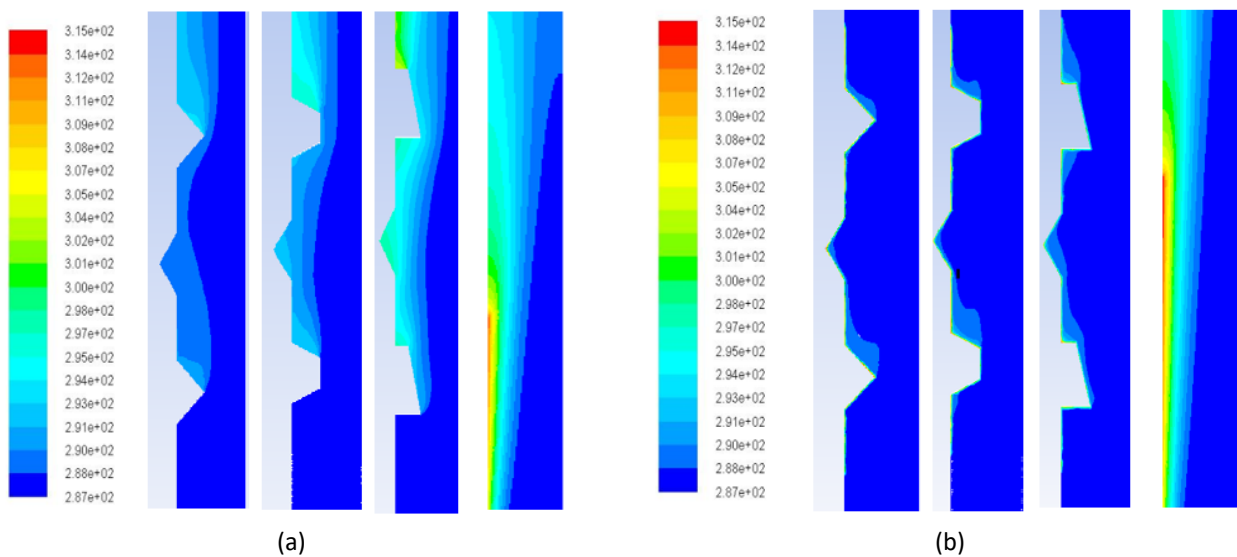
It has been noted that triangular rib-groove shape channel has provided more sufficient rate of heat transfer amongst all of ribbed channel shape types in addition to the smooth channel. Which is why the triangular shape of the rib-groove had a higher heat transfer rate of other ribs, due to the fact that it had a smallest tip and a sharp edge, which is why the leading edge area and the behavior of the trailing edge has been at the maximum value for the semi-trapezoidal shape of the rib-groove and at the minimal value for triangular shape of the rib-groove, which provides more heat transfer area and produces a higher mixing of fluid and turbulence flow compared to other ribs (i.e. the trapezoidal and the semi-trapezoidal ones). It is seen that the coefficient of the heat transfer for channel fitted with 3 rib shapes (triangle, trapezoidal, and semi-trapezoidal) has been greater compared to the smooth channel by (59% for triangle rib-fitted channel), by (56% for trapezoidal rib-fitted channel), and by (44% for semi-trapezoidal rib-fitted channel).

Figure 9(a) and 9(b), show the temperature distribution contours of three kind of ribbed channel (triangle, trapezoidal, and semi-trapezoidal). Never-the-less, velocity in the ribs-grooved walls' wrinkle seemed connected with Reynolds number's ascent. Which is why, adverse flow takes place in tailing edge which is near grooved channel ribs, in which flow is reverse major flow's direction. Increasing the velocity of the inverse flow indicates the fact that it became more troubled and it is said that the minor flow's severity expanded due to the major flow. In terms of temperature contours, the gradient change in temperature increases with the  $Re$  due to the formation of an opposite flow in the walls of the grooved basin. As a result, the mixing of cold fluid in the core with hot fluid near the channel walls increases via an increase in the  $Re$  [30]. It can be seen that the triangle rib-groove shape has the lowest temperature distribution of the other ribs. The reasons for that are the triangle rib-groove shape has the smallest tip and the sharp edge, which is why the leading edge's area and the behavior of the trailing edge has been at the maximum value for semi-trapezoid ribs-groove and at the minimum value for triangular ribs-groove shape which provides more area for the

transfer of the heat and produced a flow of turbulence which is greater than other ribs (i.e. the semi-trapezoid and the trapezoid).



**Fig. 8.** Variation of the heat transfer rate for the various ribbed groove channels shape



**Fig. 9.** Effect of Ribs groove Shape on Temperature Distribution (a) 0.105m/s and 0.263m/s (b) 0.316m/s and 1.32m/s for water and air superficial velocities at constant heat flux

#### 4.3 Heat Transfer Enhancement of Ribs-Grooved Shapes

According to the past literature studies [31, 32], a comparison of heat transfer coefficients in a smooth channel and channel with different ribs shapes was made at the same power of pumping due to the fact that it is relevant to the operational cost. The heat transfer enhancement efficiency for a constant pumping power may be defined as follows

$$\eta = (h_a/h_s)_p \quad (13)$$

$h_a$  and  $h_s$  are respectively the coefficients of the convective transfer of heat with and with no groove, and index P is the pumping power.

Figure 10 shows that the comparison between different Rib-groove channels increases the efficiency of heat transfer with different  $Re$  at constant pumping power. It has been shown from the present work that the value of heat transfer enhancement has been comparatively improved by the use of the triangle rib-groove, whereas the semi-trapezoid rib-groove form has a lower value of heat transfer improvement. It has also been found that, in the case of low Reynolds number, the value of the heat transfer enhancement factor is comparable and with the increase of the Reynolds number for all ribs-groove shapes. This is mainly attributed to the intensity of turbulence which is higher in ribs shape compared with that of smooth channels.

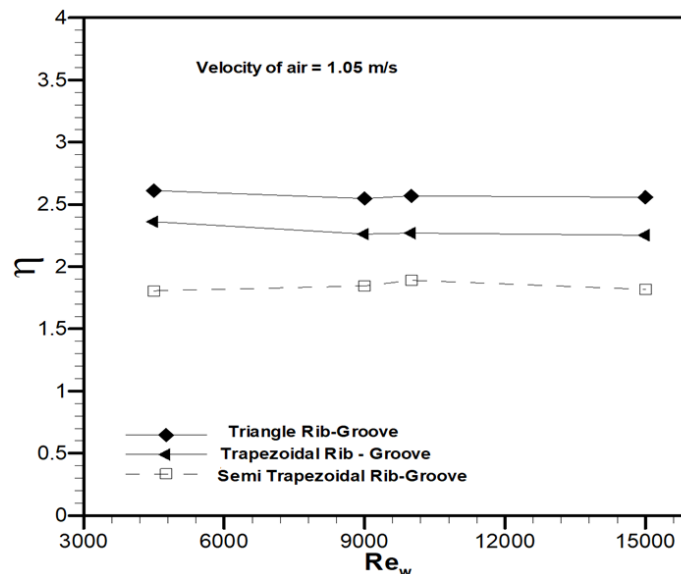


Fig. 10. Variation of enhancement efficiency of heat transfer with  $Re$  for different Rib-groove channels

#### 4. Conclusions

This work represented an experimental and theoretical analysis of forced convection heat transfer and temperature distribution over a vertically aligned rectangular ribbed channel. The concluding remarks are listed below

- i. Impacts of various ribs-groove shapes (triangular, trapezoidal, and semi-trapezoidal) at a certain air and water surface velocity value on the heat transfer behavior of the computational fluids. Increasing the mixture Reynolds number's value results in enhancing turbulent intensity which results in the enhancement of the rate of heat transfer.
- ii. On the basis of the measurements and the findings obtained, it was assumed that the rate of heat transfer increases with an increase in water and air surface velocities for rib grooves as a consequence of the creation of a thinner boundary layer for rib grooves.
- iii. By adjusting the form of the ribs – groove on the fluid and thermal fields, the results showed that the triangle rib-groove form gives the highest coefficients of heat transfer, followed by the trapezoid rib-groove, while the semi-trapezoidal rib-groove shape gives the lowest value.
- iv. The efficiency of the heat transfer enhancement in case of triangle rib-groove is higher followed by trapezoidal rib and semi trapezoidal rib-groove channel.
- v. Temperature distribution contours of three kinds of ribbed channel indicate that the velocity of the ribbed walls seemed to be related to the increase of the number of Reynolds. As a

consequence, the triangle rib-groove shape has the lowest temperature range of the other ribs.

## References

- [1] Al-Shamani, Ali Najah, K. Sopian, and H. A. Mohammed. "Sohif Mat, Mohd Hafidz Ruslan, Azher M." *Abed, Enhancement heat transfer characteristics in the channel with Trapezoidal rib-groove using nanofluids, Case Stud. Therm. Eng* 5 (2015): 48-58. <https://doi.org/10.1016/j.csite.2014.12.003>
- [2] Mohammed, H. A., Azher M. Abed, and M. A. Wahid. "The effects of geometrical parameters of a corrugated channel with in out-of-phase arrangement." *International Communications in Heat and Mass Transfer* 40 (2013): 47-57. <https://doi.org/10.1016/j.icheatmasstransfer.2012.10.022>
- [3] Oleiwi, Sarah, and Riyadh Al-Turaihi. "The effect of ribs height in two phase flow (air-water) on heat transfer coefficient in vertical ribbed duct." *Ain Shams Engineering Journal* 10, no. 4 (2019): 801-810. <https://doi.org/10.1016/j.asej.2019.01.002>
- [4] Al-Jibory, M., R. Al-Turaihi, and H. Al-Jibory. "An experimental and numerical study for two phase flow (water-air) in rectangular ducts with compound turbulators." In *IOP Conference Series: Materials Science and Engineering*, IOP Publishing. 2018. <https://doi.org/10.1088/1757-899X/433/1/012049>
- [5] Abed, Azher M., K. Sopian, H. A. Mohammed, M. A. Alghoul, Mohd Hafidz Ruslan, Sohif Mat, and Ali Najah Al-Shamani. "Enhance heat transfer in the channel with V-shaped wavy lower plate using liquid nanofluids." *Case Studies in Thermal Engineering* 5 (2015): 13-23. <https://doi.org/10.1016/j.csite.2014.11.001>
- [6] Abed, Azher M., M. A. Alghoul, K. Sopian, H. A. Mohammed, and Ali Najah Al-Shamani. "Design characteristics of corrugated trapezoidal plate heat exchangers using nanofluids." *Chemical Engineering and Processing: Process Intensification* 87 (2015): 88-103. <https://doi.org/10.1016/j.cep.2014.11.005>
- [7] Manca, Oronzio, Sergio Nardini, and Daniele Ricci. "Numerical study of air forced convection in a channel provided with inclined ribs." *Frontiers in Heat and Mass Transfer (FHMT)* 2, no. 1 (2011). <https://doi.org/10.5098/hmt.v2.1.3007>
- [8] Ansari, M. R., and B. Arzandi. "Two-phase gas-liquid flow regimes for smooth and ribbed rectangular ducts." *International Journal of Multiphase Flow* 38, no. 1 (2012): 118-125. <https://doi.org/10.1016/j.ijmultiphaseflow.2011.08.008>
- [9] San, Jung-Yang, and Wen-Chieh Huang. "Heat transfer enhancement of transverse ribs in circular tubes with consideration of entrance effect." *International Journal of Heat and Mass Transfer* 49, no. 17-18 (2006): 2965-2971. <https://doi.org/10.1016/j.ijheatmasstransfer.2006.01.046>
- [10] Pinelli, Davide, and Franco Magelli. "Analysis of the fluid dynamic behavior of the liquid and gas phases in reactors stirred with multiple hydrofoil impellers." *Industrial & engineering chemistry research* 39, no. 9 (2000): 3202-3211. <https://doi.org/10.1021/ie000216+>
- [11] Behnampour, Ali, Omid Ali Akbari, Mohammad Reza Safaei, Mohammad Ghavami, Ali Marzban, Gholamreza Ahmadi Sheikh Shabani, and Ramin Mashayekhi. "Analysis of heat transfer and nanofluid flow in microchannels with trapezoidal, rectangular and triangular shaped ribs." *Physica E: Low-Dimensional Systems and Nanostructures* 91 (2017): 15-31. <https://doi.org/10.1016/j.physe.2017.04.006>
- [12] Mohebbi, Komeil, Rohollah Rafee, and Farhad Talebi. "Effects of rib shapes on heat transfer characteristics of turbulent flow of Al<sub>2</sub>O<sub>3</sub>-water nanofluid inside ribbed tubes." *Iranian Journal of Chemistry and Chemical Engineering (IJCCE)* 34, no. 3 (2015): 61-77.
- [13] Karwa, Rajendra, S. C. Solanki, and J. S. Saini. "Heat transfer coefficient and friction factor correlations for the transitional flow regime in rib-roughened rectangular ducts." *International Journal of Heat and Mass Transfer* 42, no. 9 (1999): 1597-1615. [https://doi.org/10.1016/S0017-9310\(98\)00252-X](https://doi.org/10.1016/S0017-9310(98)00252-X)
- [14] Eiamsa-ard, Smith, and Pongjet Promvonge. "Numerical study on heat transfer of turbulent channel flow over periodic grooves." *International Communications in Heat and Mass Transfer* 35, no. 7 (2008): 844-852. <https://doi.org/10.1016/j.icheatmasstransfer.2008.03.008>
- [15] Ramadhan, Abdulmajeed A., Yaser T. Al Anii, and Amer J. Shareef. "Groove geometry effects on turbulent heat transfer and fluid flow." *Heat and Mass Transfer* 49, no. 2 (2013): 185-195. <https://doi.org/10.1007/s00231-012-1076-9>
- [16] Fathinia, Farshid, Mohammad Parsazadeh, and Amirhossein Heshmati. "Turbulent Forced Convection Flow in a Channel over Periodic Grooves using Nanofluids." *International Journal of Mechanical and Mechatronics Engineering* 6, no. 12 (2012): 2782-2787.
- [17] Sivakumar, K., E. Natarajan, and N. Kulasekharan. "Heat transfer and pressure drop comparison between smooth and different sized rib-roughened rectangular divergent ducts." *International Journal of Engineering and Technology (IJET)* 6, no. 1 (2014): 263-272.

- [18] Fifi, NM Elwekeel, MM Abdala Antar, and Zheng Qun. "Numerical investigation of heat transfer coefficient in ribbed rectangular duct with various shaped ribs and different coolants." In *Proceedings of the 1st International Conference on Mechanical Engineering and Material Science*. Atlantis Press (2012). <https://doi.org/10.2991/mems.2012.119>
- [19] Salman, Sami D. "Comparative study on heat transfer enhancement of nanofluids flow in ribs tube using CFD simulation." *Heat Transfer—Asian Research* 48, no. 1 (2019): 148-163. <https://doi.org/10.1002/htj.21376>
- [20] Kim, Dae Hyun, Byung Ju Lee, Jung Shin Park, Jae Su Kwak, and Jin Taek Chung. "Effects of inlet velocity profile on flow and heat transfer in the entrance region of a ribbed channel." *International Journal of Heat and Mass Transfer* 92 (2016): 838-849. <https://doi.org/10.1016/j.ijheatmasstransfer.2015.05.077>
- [21] Eiamsa-Ard, Smith, and Pongjet Promvonge. "Thermal characteristics of turbulent rib-grooved channel flows." *International Communications in Heat and Mass Transfer* 36, no. 7 (2009): 705-711. <https://doi.org/10.1016/j.icheatmasstransfer.2009.03.025>
- [22] Abdulrazzaq, Tuqa, Hussein Togun, M. K. AAriffin, S. N. Kazi, N. M. Adam, and S. Masuri. "Numerical simulation on heat transfer enhancement in channel by triangular ribs." *Proc. World Acad. Sci. Eng. Technol* 80 (2013): 434-438.
- [23] Habeeb, Laith Jaafer, and Riyadh S. Al-Turaihi. "Experimental Study and CFD Simulation of Two-Phase Flow Around Triangular Obstacle in Enlarging Channel." *Int. J. Eng. Res. Appl* 3, no. 4 (2013): 2036-2042.
- [24] Salameh, Tareq. "On enhancement of heat transfer with ribs." (2008).
- [25] Islam, Md Shafiqul, Ryutaro Hino, Katsuhiko Haga, Masanori Monde, and Yukio Sudo. "Experimental study on heat transfer augmentation for high heat flux removal in rib-roughened narrow channels." *Journal of nuclear science and technology* 35, no. 9 (1998): 671-678. <https://doi.org/10.1080/18811248.1998.9733923>
- [26] Ghorbani-Tari, Zahra. "Experimental investigations of heat transfer in a channel with ribs and obstacle." PhD diss., Lund University (2014).
- [27] Fluent, I. N. C. "FLUENT 6.3 user's guide." *Fluent documentation* (2006).
- [28] Jalghaf, Humam Kareem, Riyadh S. Al-Turaihi, and Jaafer Habeeb. "Air-water flow investigation around hot circular cylinder inside channel." *Advances in Natural and Applied Sciences* 10, no. 12 (2016): 16-28.
- [29] Nada, S. A. "Experimental Investigation and Empirical Correlations of Heat Transfer in Different Regimes of Air–Water Two-Phase Flow in a Horizontal Tube." *Journal of Thermal Science and Engineering Applications* 9, no. 2 (2017). <https://doi.org/10.1115/1.4034903>
- [30] Ajeel, Raheem K., WS-IW Salim, and Khalid Hasnan. "Thermal and hydraulic characteristics of turbulent nanofluids flow in trapezoidal-corrugated channel: Symmetry and zigzag shaped." *Case studies in thermal engineering* 12 (2018): 620-635. <https://doi.org/10.1016/j.csite.2018.08.002>
- [31] Zimparov, Ventsislav. "Enhancement of heat transfer by a combination of three-start spirally corrugated tubes with a twisted tape." *International Journal of Heat and Mass Transfer* 44, no. 3 (2001): 551-574. [https://doi.org/10.1016/S0017-9310\(00\)00126-5](https://doi.org/10.1016/S0017-9310(00)00126-5)
- [32] Promvonge, Pongjet. "Thermal performance in circular tube fitted with coiled square wires." *Energy Conversion and Management* 49, no. 5 (2008): 980-987. <https://doi.org/10.1016/j.enconman.2007.10.005>